Electron Mobilities of n-Type Organic Semiconductors from Time-Dependent Wavepacket Diffusion Method: Pentacenequinone Derivatives

ARTICLE *in* THE JOURNAL OF PHYSICAL CHEMISTRY A · APRIL 2012

Impact Factor: 2.69 · DOI: 10.1021/jp3023474 · Source: PubMed

3 AUTHORS, INCLUDING:

Weiwei Zhang
University of Science and Technology of China
8 PUBLICATIONS **85** CITATIONS
SEE PROFILE

Yi Zhao
Xiamen University
89 PUBLICATIONS **1,165** CITATIONS
SEE PROFILE

THE JOURNAL OF PHYSICAL CHEMISTRY A

Article

pubs.acs.org/JPCA

Electron Mobilities of n-Type Organic Semiconductors from Time-Dependent Wavepacket Diffusion Method: Pentacenequinone Derivatives

WeiWei Zhang, XinXin Zhong, and Yi Zhao*

State Key Laboratory for Physical Chemistry of Solid Surfaces, Fujian Provincial Key Laboratory of Theoretical and Computational Chemistry, College of Chemistry and Chemical Engineering, Xiamen University, Xiamen, 361005, People's Republic of China

Supporting Information

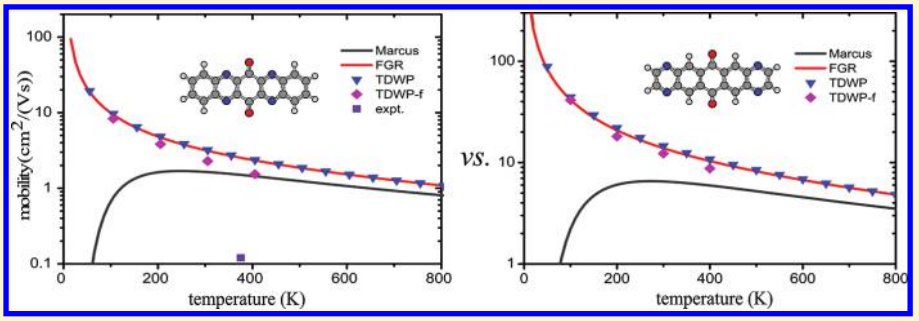

ABSTRACT: The electron mobilities of two n-type pentacenequinone derivative organic semiconductors, 5,7,12,14-tetraaza-6,13-pentacenequinone (TAPQ5) and 1,4,8,11-tetraaza-6,13-pentacenequinone (TAPQ7), are investigated with use of the methods of electronic structure and quantum dynamics. The electronic structure calculations reveal that the two key parameters for the control of electron transfer, reorganization energy and electronic coupling, are similar for these two isomerization systems, and the charge carriers essentially display one-dimensional transport properties. The mobilities are then calculated by using the time-dependent wavepacket diffusion approach in which the dynamic fluctuations of the electronic couplings are incorporated via their correlation functions obtained from molecular dynamics simulations. The predicted mobility of TAPQ7 crystal is about six times larger than that of TAPQ5 crystal. Most interestingly, Fermi's golden rule predicts the mobilities very close to those from the time-dependent wavepacket diffusion method, even though the electronic couplings are explicitly large enough to make the perturbation theory invalid. The possible reason is analyzed from the dynamic fluctuations.

1. INTRODUCTION

Organic semiconductors have attracted a widespread attention during the past decades due to their great potential advantages, such as low-cost, large-area coverage, flexibility and ease of processing.[1−6] Many kinds of p-type organic semiconductors with high-performance have been fabricated,[7] and applied to design organic thin-film transistors (OTFTs).[8] However, the development of n-type organic semiconductors lags behind the p-type ones due to the instability of organic anions in the presence of air and water, weak electron injection, and unfavorable electron mobility. As n-type organic materials apply to p−n junction diodes, organic solar cells, and so on,[5] theoretical investigation for electron transport is helpful in the design of high-performance n-type materials and, thus, becomes more and more important.

In general, a strategy of designing n-type organic semiconductors is adding electron-withdrawing groups or substituents, such as fluorine, bromine, cyano, and imide moieties, to lower the energy of the lowest unoccupied molecular orbital (LUMO) and provide strong electron affinities. Based on this hint, a serious of n-type organic semiconductors have been synthesized (see, for instance, refs 7 and 9). Recently, Mamada et al.[10,11] have shown that the quinone n-type organic semiconductors have high electron affinities, and their molecular arrangements are relatively easily prepared and controlled. They have developed the n-type OTFT based on novel anthraquinones as quinones, and the largest electron mobility is up to 0.074 $cm^2/(Vs)$.[10] The mobility is further increased to 0.15 $cm^2/(Vs)$ by choosing Benzo[1,2-b:4,5-b′]-dithiophene-4,8-dione derivative as a quinone moiety.[11] Tang and Liang et al. have synthesized a series of Nitrogen-rich heteroquinones and fluorinated pentacenequinones.[12,13] In those n-type materials, there are two isomers: 5,7,12,14-tetraaza-6,13-pentacenequinone (TAPQ5, shown in Figure 1) and 1,4,8,11-tetraaza-6,13-pentacenequinone(TAPQ7, Figure 2). Their mobilities measured from the experiments are in the range of 0.05−0.12 $cm^2/(Vs)$[12] and $2-6 \times 10^{-5}$ $cm^2/(Vs)$,[13] respectively. Although the mobility of TAPQ7 is 3

Special Issue: Jörn Manz Festschrift

Received: March 11, 2012
Revised: April 6, 2012

   dx.doi.org/10.1021/jp3023474 | J. Phys. Chem. A XXXX, XXX, XXX−XXX

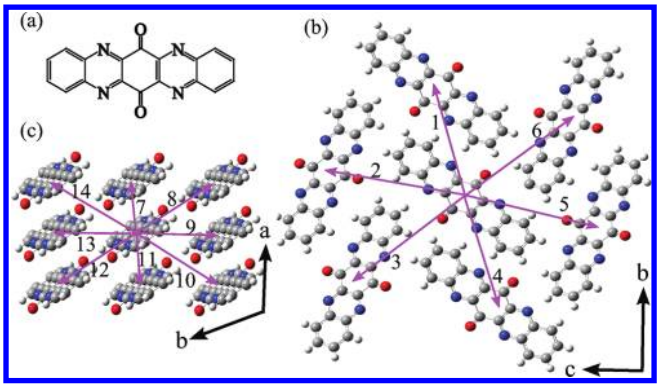

Figure 1. (a) Chemical structure of TAPQ5. (b) Crystal structure in the *bc* plane. (c) Crystal structure in the *ab* plane (a = 3.89 Å, b = 9.07 Å, c = 18.43 Å, β = 92.3° for unit cell). The Arabic numerals correspond to the types of molecular pairs used in the calculations of electronic couplings.

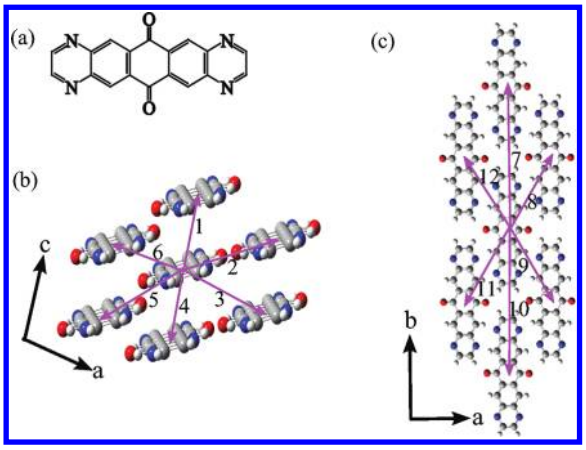

Figure 2. (a) Chemical structure of TAPQ7. (b) Crystal structure in the *ac* plane. (c) Crystal structure in the *ab* plane (a = 10.59 Å, b = 16.04 Å, c = 3.80 Å, β = 95.6° of unit cell). The labels correspond to the types of molecular pairs used in the calculations of electronic couplings.

order lower than that of TAPQ5, the molecular packing of TAPQ5 and TAPQ7 crystals has a similar π-stacking and quadruple weak H-bonds. The possible reason for such a large difference has been explained by the different morphologies that TAPQ5 has a polycrystalline film whereas TAPQ7 forms an amorphous film.[13] Indeed, the mobilities strongly depend on the morphology and can cover several orders of magnitude from highly disordered amorphous films to highly ordered materials.[14]

In the present paper, we theoretically calculate the mobilities in TAPQ5 and TAPQ7 crystals to predict the possible ultimate values that the experiments can reach and understand how the isomer structures influence the electron mobilities. A simple method to calculate the mobility is starting from Marcus formula to estimate electron transfer (ET) rate, in which the mobility is evaluated from Einstein relation by using the ET rate between two monomers in crystal.[15,16] To obtain the ET rate, the two key parameters, electronic coupling and reorganization energy, are calculated from electronic structure theory. Although this simple method has successfully applied to many organic semiconductors, it has the intrinsic limits and sometimes predicts an incorrect temperature dependence of mobility.[17,18] One of limitations is that the dynamic disorder of the electronic coupling caused by the structural fluctuation of crystal is not involved in ET. This limit can be overcome by using Monte Carlo simulations or the master equation method.[19,20] Another explicit limit is that the Marcus rate formula is only suitable to the systems with weak electronic couplings and at high temperatures. Therefore, this method is applicable for the hopping-type mobility. As the electronic coupling becomes strong, one may still use the improved ET rates[21] to predict the hopping-type mobility. In organic semiconductors, however, the electronic coherence motion among several monomers may begin to play a role, that is, the mobility follows the mechanism of bandlike transport. To incorporate the effects of both the electronic coherence motion and structural fluctuation of crystal on the mobility, one has to simultaneously propagate electronic wave function or density matrix and nuclear motions of crystal. Trois et al.[22−24] have suggested a mixed quantum-classical method in which the time-dependent Schrödinger equation is used to describe the electronic motion and the nuclear motions are solved by using the Newton equation. To incorporate the quantum effect of the nuclear motions, several quantum approaches have been also proposed. For instance, the mobility expression has been derived based on the Holstein−Peierls model.[25,26] The Redfield theory and its improvements[27] have also been used to predict the charge mobility. Recently, the nonperturbative quantum master equation approach is applied to obtain the charge mobility.[28−31] The multilayer multiconfiguration time-dependent Hartree method has been applied extensively to deal with the heterogeneous charge transfer process within hundreds to thousands of electronic states.[32−34] We have also extended the path integral method originally proposed by Makri's group[35−37] to investigate the coherent motions of charge carrier.[38,39]

In this paper, we use the time-dependent wavepacket diffusion (TDWPD) method proposed by us recently to calculate the mobility.[40] This approach is originally based on the Haken−Strobl−Reineker (HSR) model where the fluctuations of the monomer energies and electronic couplings are dealt with the classical stochastic fields.[41−46] We have extended the model to solve the electron motion by the wavepacket method and obtain the time-dependent fluctuations of the monomer energies and electronic couplings from the corresponding spectral density functions. The TDWPD method has a similar simulation cost to the mixed quantum-classical method, however, it partially includes the quantum effect caused by the nuclear motions, and also incorporates the memory effect of the electronic coupling fluctuation.[40] Furthermore, compared to most available quantum methods that are still limited to tens of monomers because of the challenge of numerical convergence, it can be easily used to handle the systems with thousands of monomers (nanoscale).

To predict the mobility with use of the TDWPD approach, we need to know the electron−phonon interaction and fluctuation of the electronic couplings. The fluctuation is generated from the time-dependent correlation function which are obtained by the electronic structure theory calculations and the molecular dynamics (MD) simulations.[40,47] Although the fluctuations are corresponding to two adjacent monomers, we have implemented the MD simulations on the crystals with the periodic boundary conditions to incorporate the environment effect on the electronic couplings.[18]

The paper is arranged as follows. Section 2 describes the working expression of the time-dependent wavepacket diffusion approach. The electronic structure methods for the calculations

dx.doi.org/10.1021/jp3023474 | J. Phys. Chem. A XXXX, XXX, XXX−XXX

of reorganization energy and electronic coupling are also summarized. Section 3 shows the results and discussion. The concluding remarks are presented in section 4.

2. CALCULATED METHODS

2.1. Time-Dependent Wavepacket Diffusion Method. As an electron is injected to a monomer in the crystal, it hops or coherently moves to other monomers, and its transfer rate is determined by the electronic energies of the monomers (sites) and the couplings between the sites. In organic crystals, the times of nuclear motions and electron transfer commonly have a similar order. Therefore, the electronic coupling between sites and site energies are fluctuated during the ET. Based on the HSR model, the electronic Hamiltonian incorporated those fluctuations can be modeled as follows[44,48]

$$H(t) = \sum_{i=1}^{N} (\varepsilon_{ii} + V_{ii}(t))|i\rangle\langle i| + \sum_{i\neq j}^{N} (\varepsilon_{ij} + V_{ij}(t))|i\rangle\langle j| \quad (1)$$

where $|i\rangle$ represents the electronic state of the ith site, ε_{ii} and ε_{ij} are the site energy and electronic coupling at the stable structure of the crystal, and $V_{ii}(t)$ and $V_{ij}(t)$ correspond to the fluctuations caused by the nuclear motions in the crystal. To incorporate the memory effect of the site energy fluctuation, we start from the spectral density function of the electron−phonon interaction[49]

$$J(\omega) = \frac{\pi}{2}\sum_{j}\frac{c_j^2}{\omega_j}\delta(\omega - \omega_j) \quad (2)$$

Here, c_j and ω_j represent the electron−phonon interaction and frequency of the jth normal mode, respectively. c_j can be calculated by $\omega_j^2\Delta Q_j$, where ΔQ_j is the mode coordinate shifts during ET. The ω_j and ΔQ_j can be calculated from the electronic structure method (see the next subsection). Once $J(\omega)$ is known, the site energy fluctuation can be obtained by[50]

$$V_{ii}(t) = \sqrt{2}\sum_{i=1}^{N}[2G(\omega_n)\Delta\omega]^{1/2}\cos(\omega_n t + \phi_n) \quad (3)$$

Here, $G(\omega)(\equiv J(\omega)\coth(\beta\omega/2)/\pi)$ is the modified spectral density function at a given temperature T ($\beta = 1/k_BT$) to make it satisfy the detailed-balance principle.[40,47] $\Delta\omega = \omega_{max}/N$, where ω_{max} is the upper cutoff frequency. $\omega_n = n\Delta\omega$ and ϕ_n are the independent random phases which are uniformly distributed over the interval $(0, 2\pi)$.

The fluctuation of electronic coupling is related to the correlation function, which can be calculated from $C_{cl}(t) = \langle\delta V_{ij}(t)\delta V_{ij}(0)\rangle$, where $\langle\rangle$ represents the thermal average, and $\delta V_{ij}(t)$ is the deviation of the electronic coupling from its average value $\langle V_{DA}\rangle$. The spectral density function $G_{cl}(\omega)$ is thus obtained from the Fourier transform of $C_{cl}(t)$. To incorporate the quantum effect, one may modify $G_{cl}(\omega)$ by[51]

$$G(\omega) = \frac{2G_{cl}(\omega)}{1 + e^{-\beta\omega}} \quad (4)$$

Furthermore, the fluctuation of electronic coupling satisfying the detailed-balance principle is finally generated from eq 3 together with eq 4.

To describe the electronic dynamics, the remaining task is to solve the time-dependent Schrödinger equation with the time-dependent Hamiltonian of eq 1 and it can be treated with Chebyshev polynomial expansion technique.[40,52] Once the wave function $\psi(t) = \sum_i^N c_i(t)|i\rangle$ is known, the time-dependent quantities of electron dynamics can be easily obtained. Furthermore, the charge mobility can be calculated by the Einstein relation $\mu(T) = eD(T)/k_BT$,[53] in which the diffusion coefficient $D(T)$ is given by

$$D(T) = \lim_{t\to\infty}\frac{\langle q^2(t)\rangle}{2dt} \quad (5)$$

where d is the dimension of the system, and $\langle q^2(t)\rangle$ is the mean-squared displacement of electron motion, which is calculated from[40]

$$\langle q^2(t)\rangle = \sum_i \langle\psi(t)|i^2|\psi(t)\rangle l^2 = \sum_i \rho_{ii}(t)i^2l^2 \quad (6)$$

Here l is the distance of two adjacent molecule sites and $\rho_{ii}(t) = \langle c_i^*(t)c_i(t)\rangle$ is the electron population on the ith site .

2.2. Computational Methods for Reorganization Energy and Electronic Coupling. In this section, we outline the methods for the calculations of the electron−phonon interaction and electronic coupling. It has been shown that the electron−phonon interaction coefficient c_j in the spectral density function of eq 2 is related to the coordinate shift ΔQ_j by $\omega_j^2\Delta Q_j$. On the other hand, the reorganization energy can also be calculated from ω_j and ΔQ_j by

$$\lambda = \sum_j \lambda_j = \sum_j \frac{1}{2}\omega_j^2\Delta Q_j^2 \quad (7)$$

ω_j and ΔQ_j are determined from electronic structure calculations for realistic organic crystals. In the numerical implementation, we first find the two optimized electronic states of $|M^-M\rangle$ and $|MM^-\rangle$, where M is a monomer. The normal-mode analysis is then made on both states in the same normal mode coordinates. The frequency ω_j is thus automatically given out and the coordinate shift ΔQ_j is projected out from the shifts of the molecular rectangular-coordinates by a matrix transform technique. The detailed numerical calculation method is referred to, for instance, refs 18 and 21.

Compared to the electron−phonon interaction calculation, the accurate method to calculate the electronic coupling is not well established yet, although a number of computational approaches have been proposed to evaluate it,[54] such as, Koopmans' theorem method (KT),[55−58] the two-state model (TM),[59] the spin-flip (SF) strategy,[60] the generalized Mulliken-Hush (GMH) method,[61] and the reduced TM (RTM).[18,62] KT is the simplest method, which assumes that the electron transport is related to LUMO of the organic molecule in n-type materials. The electronic coupling thus equals to a half electronic energy split between LUMO and LUMO+1 of the dimer. However, it is only valid when the site energies of both monomers are equal.[18] TM can predict the reasonable electronic coupling; however, it is not easy to numerically determine two diabatic states at a given geometry of dimer obtained from MD simulation. In the present work, the RTM method is used to overcome the limit of KT and the difficulty of TM.

Similar to TM, the electronic coupling is still calculated from the overlap of the two diabatic states in the RTM, but the diabatic states are assumed to be the LUMOs of two isolated neutral monomers borrowed from the KT mechanism. In this case, the secular equation in the diabatic representation is

dx.doi.org/10.1021/jp3023474 | J. Phys. Chem. A XXXX, XXX, XXX−XXX

$$\begin{pmatrix} h_{11} & h_{12} \\ h_{21} & h_{22} \end{pmatrix} C = E \begin{pmatrix} 1 & S_{12} \\ S_{21} & 1 \end{pmatrix} C \tag{8}$$

where $h_{ij} = \langle \phi_i | h_{KS} | \phi_j \rangle$, $S_{ij} = \langle \phi_i | S | \phi_j \rangle$, and $|\phi_i\rangle$ $(i = 1, 2)$ is the electronic wave function of LUMO for the ith monomer. These quantities can be calculated from the Kohn–Sham (KS) or Hartree–Fock (HF) equation. After the transformation of eq 8 into the orthogonal basis set,[18,62,63] the electronic coupling is given by

$$V_{DA} = \frac{h_{12} - \frac{1}{2}(h_{11} + h_{22})S_{12}}{1 - S_{12}^2} \tag{9}$$

and the corresponding site energies are

$$H_{11(22)} = \frac{(h_{11} + h_{22}) - 2h_{12}S_{12} \pm (h_{11} - h_{22})\sqrt{1 - S_{12}^2}}{2(1 - S_{12}^2)} \tag{10}$$

It is interesting to note that the RTM predicts both the electronic coupling and the site energies. Together with the MD simulation, one can thus simultaneously obtain the fluctuations of the electronic coupling and site energies. The later may act as an alternative way to generate the site energy fluctuation.

2.3. Electronic Structure Methods. For the isolated TAPQ5 and TAPQ7 molecules, the density functional theory (DFT) with different functionals are used to optimize geometries. The obtained structural parameters for these two molecules are listed in the Supporting Information. It is found that the hybrid functional PBE1PBE/6-31+G* among the tested functionals predicts the results closest to the experimental ones. Therefore, this functional is used to calculate the electron–phonon interactions and reorganization energies. In the calculations of electronic couplings, however, we choose the PW91 exchange and PW91 correlation functionals with 6-31G* basis set, which has been demonstrated to have a good description for electronic coupling at the DFT level.[18,64] All the calculations are manipulated by the Gaussain 09 suite.[65]

To obtain the structural fluctuation of the crystal, MD simulations with periodic boundary conditions are carried out by the Tinker 5.1 molecular modeling package.[66−68] We construct the 8 × 4 × 3 supercell with 192 molecules and the 5 × 5 × 8 supercell consisting of 200 molecules for TAPQ5 and TAPQ7, respectively. The intra- and intermolecular interactions are described by an all-atoms force field based on the OPLS parameters (OPLSAA),[69] which has been demonstrated to be suitable for the organic semiconductors.[70,71] The MD simulation is performed in the NVT ensemble with an Andersen thermostat. The equation of motion is integrated by the Verlet algorithm with a time step of 2 fs. The hydrogen bonds are constrained to an ideal bond length with the help of the RATTLE algorithm. After the equilibration, a succeeding simulation of 120 ps is run and 6000 snapshots of the geometry are extracted for the calculation of the electronic coupling.

3. RESULTS AND DISCUSSION

3.1. Reorganization Energy and Electronic Coupling. Because the fluctuation of site energy is generated from the electron–phonon interaction, we first focus on the mode-specific reorganization energy λ_i in eq 7, which is related to the strength of the electron–phonon interaction and can make chemists easily understand the ET mechanism from conventional ET theory. Figure 3 displays the frequency dependence

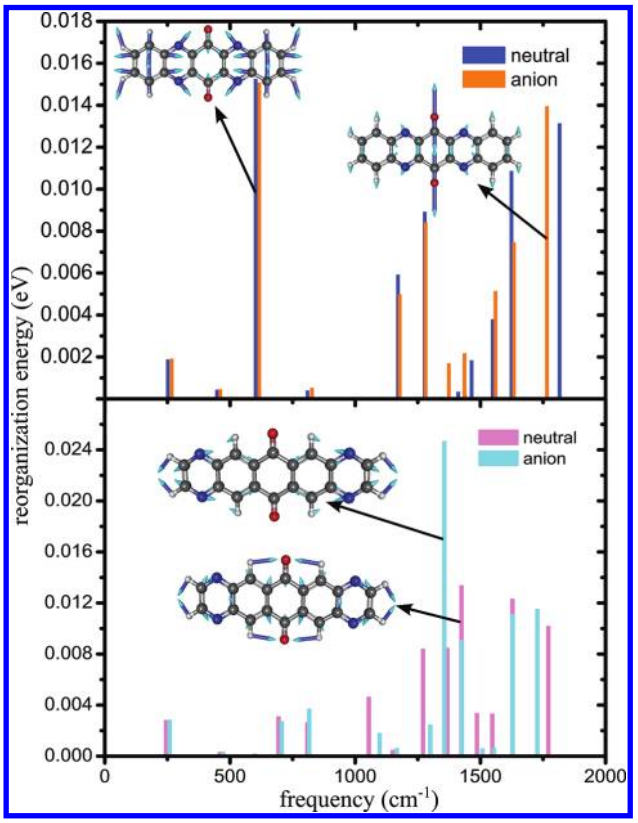

Figure 3. Frequency dependence of mode-specific reorganization energies for TAPQ5 (above) and TAPQ7 (below). Neutral and anion represent the reorganization energies for neutral and anionic states, respectively. The insets show the normal modes with large contributions.

of the mode-specific reorganization energies for TAPQ5 and TAPQ7. It is shown that only several normal modes have the large contributions to the total reorganization energies for both systems, and the corresponding frequencies are relatively high. One thus expects that the vibrational quantum effect on ET should be explicit. Indeed, the effective frequencies ω_{eff} calculated from the formula[54,72]

$$\omega_{eff} = \sqrt{\frac{\sum_i \omega_i^2 \lambda_i}{\sum_i \lambda_i}} \tag{11}$$

are 1352.8 and 1418.5 cm^{-1} for TAPQ5 and TAPQ7, respectively, and $\hbar\omega_{eff}/k_BT \gg 1$ at room temperature.

To confirm the accuracy of the mode-specific reorganization energies, we also employ the four-point approach[73] to estimate the total reorganization energy, which can be directly used to compare with the one from the summation of mode-specific reorganization energies. The four-point method is very easy to implement, and it has been identified as a reliable tool by our previous studies on the ET processes.[18,54] The obtained total reorganization energies from the four-point approach are 125.1 and 146.0 meV for TAPQ5 and TAPQ7, respectively. Alternatively, the predicted total reorganization energies from eq 7 are 125.3 and 146.8 meV, respectively. The two methods predict the surprisedly consistent results, manifesting the mode-specific reorganization energies are quite accurate and the

dx.doi.org/10.1021/jp3023474 | J. Phys. Chem. A XXXX, XXX, XXX−XXX

Table 1. Electronic Couplings for Different Molecular Pairs in TAPQ5 and TAPQ7 Crystals

		1	2	3	4	5	6	7	8	9	10	11	12	13	14
TAPQ5	r^a	9.07	10.39	10.52	9.07	10.38	10.32	3.89	9.87	9.07	9.87	3.89	9.87	9.07	9.87
	$V_{DA}{}^b$	9.58	5.54	5.97	9.58	5.54	5.97	63.76	2.08	9.58	0.02	63.76	2.08	9.58	0.02
TAPQ7	r	3.80	10.14	9.61	3.80	10.14	9.61	16.03	9.61	9.61	16.03	9.61	9.61		
	V_{DA}	141.2	3.08	6.45	141.2	3.08	6.45	5.69	6.45	6.45	5.69	6.45	6.45		

[a]The distance between two adjacent monomers and the unit is Å. [b]The electronic coupling calculated with RTM method and the unit is meV.

harmonic oscillator approximation is valid to describe the molecular nuclear motions.[18]

It is known that the electronic couplings are dependent on the molecular arrangement. Therefore, we have to calculate the individual electronic couplings for all types of molecular pairs to determine the direction of electron transport. There are 14 and 12 types of molecular pairs in the TAPQ5 and TAPQ7 crystals, respectively, as shown in Figures 1 and 2. The values of electronic coupling for all pairs are listed in Table 1. It is found that the electronic coupling along the *a*-axis (types 7 and 11) for TAPQ5 crystal is 63.76 meV, more than 6 fold in comparison with those along other axes, and along the *c*-axis (types 1 and 4) for TAPQ7 crystal is 141.2 meV, which is 20 times larger than those along others, manifesting that the mobility for each crystal is dominantly determined to one-dimensional charge transport.

Now we focus on the fluctuations of the electronic couplings along those dominant charge transport directions. With the fluctuated geometries of the dimers from MD simulations at several temperatures (100, 200, 300, and 400 K), we have calculated the time-dependent electronic couplings, and the corresponding thermal averaged electronic couplings of TAPQ5 and TAPQ7 are listed in Table 2. As expected, the

Table 2. Thermal Averaged Electronic Couplings at Different Temperatures for TAPQ5 and TAPQ7 Crystals

	100 K	200 K	300 K	400 K
TAPQ5	78.49[a]	77.68	74.91	72.82
TAPQ7	139.83	133.04	131.65	127.45

[a]The unit of electronic coupling is meV.

average electronic couplings at low temperature (100 K) are close to those at the experimental geometries of the crystals because the fluctuated geometries are not far from the stable ones. These results manifest that the OPLSAA force field is reasonable to describe the molecular interactions for the present crystals. It is also interesting to find that the averaged electronic couplings decrease with an increase in temperature, explicitly different from our previous investigations for other organic semiconductor.[18] This phenomena may be explained by the Gaussian-type dependence of the electronic coupling with respect to the distance of two monomers. We are more interested in the correlation functions of the electronic couplings because they can straightforwardly generate the dynamic fluctuations used in the mobility calculations with TDWPD approach. Figure 4 shows the corresponding correlation functions normalized to 1 at time zero for TAPQ5 and TAPQ7, respectively. It is seen that the fluctuations for both systems show the explicit memory effect and they are nearly independent of temperatures. The fluctuation period for TAPQ5 is about 1100 fs, obviously larger than 600 fs of TAPQ7. We will show the effect of this difference on the mobility in the next section.

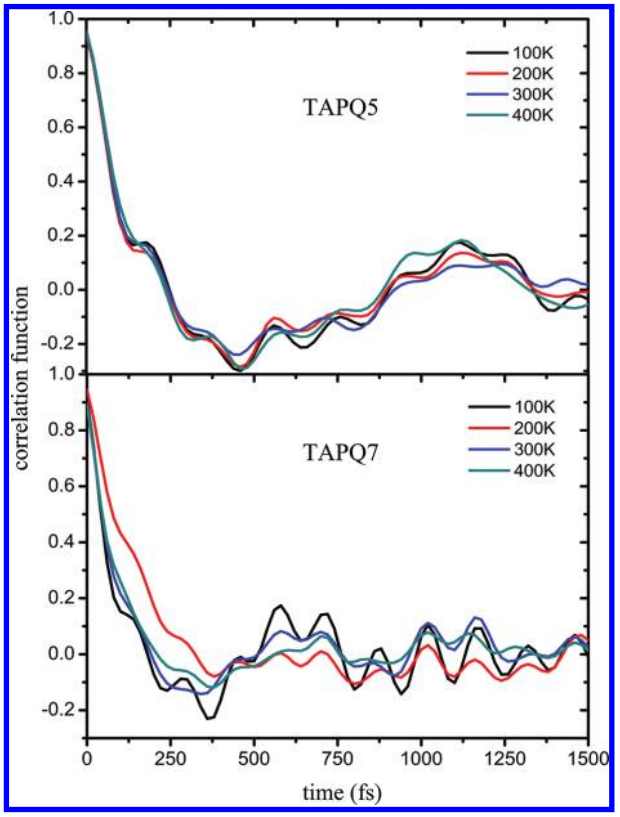

Figure 4. Correlation functions of the electronic coupling fluctuations for two crystals at different temperatures.

3.2. Mobility. It is now ready to calculate the mobilities with TDWPD approach by using the obtained fluctuations of site energies and electronic couplings calculated from electronic structure methods. Figure 5 displays the temperature dependencies of the mobilities for the TAPQ5 and TAPQ7 crystals. For a purpose of comparison, we also show the mobilities with use of thermal averaged electronic couplings, that is, not considering the fluctuation of electronic couplings. It is seen that the mobilities with the fluctuations of the electronic couplings become small compared to those from the thermal averaged electronic couplings for both TAPQ5 and TAPQ7, which are consistent with previous investigations.[23,74] Interestingly, the decrease of mobility for TAPQ5 is more explicit than that for TAPQ7, manifesting that the mobility becomes smaller with larger memory time of the fluctuation since the period for TAPQ5 is about 2 times longer than that for TAPQ7, as discussed in the last section.

From Figure 5, we further find that the two systems exhibit the bandlike charge transport properties, which generally directs to the coherence motion of electron among several sites. However, is has been shown[17,18] that the nuclear tunneling effect can also predict a bandlike property of the mobility in the hopping model, where the electron is localized

dx.doi.org/10.1021/jp3023474 | J. Phys. Chem. A XXXX, XXX, XXX−XXX

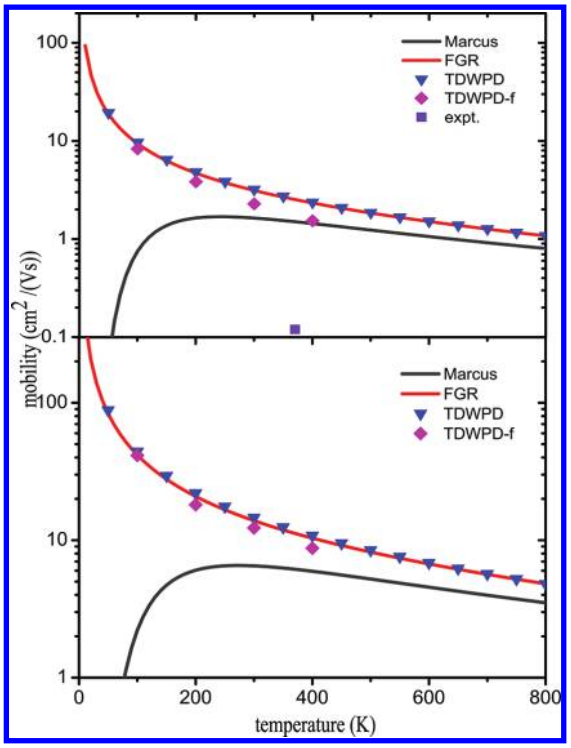

Figure 5. Temperature dependence of electron mobilities (μ) in TAPQ5 (above) and TAPQ7 (below) crystals, respectively. Marcus and FGR represent the mobilities obtained from the ET rate with eqs 13 and 15, respectively. TDWPD and TAWPD-f correspond to the mobilities from the time-dependent wavepacket diffusion approach without and with the fluctuations for electronic couplings. Expt. represents the measured mobility at 100 °C.

on one site rather than coherently delocalized among several sites, and jumps from one site to another during its transport. To judge whether this kind of bandlike property is coming from the coherence motion or nuclear tunneling effect, we also calculate the mobilities from the hopping model with the ET rate based on the perturbation theory. In this model, the mobility is still given by Einstein relation, but the diffusion coefficient is related with the ET rate by

$$D(T) = l^2 k(T)/2 \tag{12}$$

where $k(T)$ is the ET rate. At the high temperature limit, $k(T)$ is given by the well-known Marcus formula[75,76]

$$k = \frac{1}{\hbar} V_{DA}^2 \sqrt{\frac{\pi}{\lambda k_B T}} \exp\left[-\frac{(\Delta G + \lambda)^2}{4\lambda k_B T}\right] \tag{13}$$

where V_{DA} is the electronic coupling, λ is the total reorganization energy, and ΔG is the driving force. As the nuclear tunneling is incorporated, the Marcus formula can be replaced by

$$k = \frac{V_{DA}^2}{\hbar^2} \int_{-\infty}^{+\infty} dt \exp\left\{-\frac{i}{\hbar}\Delta G t - \sum_i S_i[(2n_i + 1) - n_i e^{-i\omega_i t} - (n_i + 1)e^{i\omega_i t}]\right\} \tag{14}$$

where $n_i = 1/(e^{\beta\omega_i} - 1)$ and $S_i = \lambda_i/\hbar\omega_i$ is the Huang−Rhys factor. For the symmetric ET reaction, $\Delta G = 0$. In the practical calculations, one commonly uses the approximation of a one-effective mode. In this case, eq 14 derived from the Fermi's golden rule (FGR) can be analytically carried out and the ET rate is given by[77]

$$k = \frac{2\pi V_{DA}^2}{\hbar^2 \omega}\left(\frac{n+1}{n}\right)^{p/2} \exp[-S(2n+1)] I_p\{2S[n(n+1)]^{1/2}\} \tag{15}$$

where $p = \Delta G/\hbar\omega$ and I_p is the modified Bessel function. This single mode method has been demonstrated to successfully predict the rigorous ET rate calculated from eq 14, especially for the mode having a high frequency.[47,78,79]

For a purpose of comparison, the mobilities obtained from the hopping model are also displayed in Figure 5. Surprisingly, the mobilities from the FGR for both systems have bandlike properties, and they are essentially the same as those from TDWPD method with use of thermal-averaged electronic couplings. Because the mobility from the FGR represents the hopping-type mechanism, we thus conclude that the band-like property is not from the coherence motion of electron but from the nuclear tunneling effect. Furthermore, the mobility predicted by Marcus formula, in which the nuclear tunneling effect is neglected, is much smaller than that predicted with FGR, and Marcus formula even changes the band-like transport property into a thermally activated one.

Although the mobilities from the FGR and TDWPD methods are very close to each other, we find $4V_{DA}/\lambda > 1$, from the values of the electronic coupling and reorganization energy (for instance, the ratio is about 4 for TAPQ7). Such a large ratio should lead to the delocalized property of electron, and the FGR is explicitly invalid, which is opposite to our numerical result. To analyze why the FGR is still applicable to the present systems, we compare the ET rate with the period of vibrational motions. For instance, the vibrational period is 23 fs and the inverse of the ET rate is 10 fs for TAPQ7. Although the nuclei moves slower than the electron, they are in the same order. Therefore, one expects that the vibrational motions will play an important role in the electron transfer process and it will influence the ET rates. As a result, the site energy fluctuation caused by the vibrational motions is fast enough to break down the electronic coherence between two adjacent sites; in other words, as the electron moves from the donor to the acceptor, it will be trapped in the acceptor state because of the fast fluctuations of site energies and it cannot transfer back to the donor state to perform the coherence motion. In this situation, the ET process becomes a single forward process without coherence, which may be described well by the perturbation theory. To further confirm the correctness of this analysis, we display the population propagation of the electron from the TDWPD approach (the results are shown in the Supporting Information). Indeed, the population decays with a single exponential form without any oscillator behavior. With one-fifth of the effective vibrational frequency, the coherence motion of the electron indeed appears, and the mobility from the FGR is about 4 times smaller than that from the TDWPD approach.

Finally, we propose that the theoretical mobilities at 400 K for TAPQ5 and TAPQ7 crystals are 1.54 and 8.75 cm^2/(Vs), respectively. The predicted mobility of TAPQ7 is about six times larger than that of TAPQ5. Therefore, one expects that the isomerized structure has an explicit effect on the mobility. Furthermore, compared the predicted mobilities to the experimental values for TAPQ5,[12] the predicted mobility is

dx.doi.org/10.1021/jp3023474 | J. Phys. Chem. A XXXX, XXX, XXX−XXX

about 10 times larger, and the difference comes from the fact that the theoretical mobility is for the ideal monocrystalline, whereas the measured one is for polycrystalline. It also manifests that the experimental mobility has a space to be further improved for the TAPQ5 crystal. For TAPQ7, however, the predicted mobility is much larger than the experimental value, which is in the range of $2-6 \times 10^{-5}$ $cm^2/(Vs)$.[13] Such a small experimental value has been explained by the amorphous film of TAPQ7 with the help of X-ray diffraction patterns.[13] Therefore, one expects that once the monocrystalline film of TAPQ7 is synthesized, there should be a great improvement of the mobility, and TAPQ7 should have a higher mobility than that of the TAPQ5 crystal.

4. CONCLUDING REMARKS

We have theoretically investigated the electron transfer mechanism and calculated the mobilities of two pentacenequinone derivative organic semiconductors, TAPQ5 and TAPQ7 crystals. The electronic dynamics is described by the time-dependent wavepacket diffusion approach recently proposed by us. The parameters controlling electron transfer, the reorganization energy, and electronic coupling, as well as the electron−phonon interaction, have been obtained by employing electronic structure methods. The fluctuation of electronic coupling is dealt with MD simulations. The results show that the charge carriers in two crystals display one-dimensional transport properties, and several high-frequency modes (most modes greater than 1000 cm^{-1}) control electron transfer. Although the electronic couplings are large enough to make the perturbation theory invalid, surprisingly, the perturbation theory can correctly predict the mobilities. The possible reason has been analyzed from the same order of the vibrational period and the inverse of the ET rate, and such a relatively fast vibrational motion breaks down the coherent motion of the electron between the adjacent sites and makes the electron transfer occur with a single hopping process, in which the electron only transfers from donor to acceptor without the backward transfer. In spite of the hopping-type motion of the electron, the mobility has a band-like property, which has been explained by the large nuclear tunneling effect. Furthermore, the predicted mobility of TAPQ7 is about six times larger than that of TAPQ5. Compared to the measured values, the theoretically predicted mobilities are much higher, suggesting that the experimental mobilities may be further increased by synthesizing pure crystalline films. The results may be helpful for experimentalists to choose the candidate isomeric materials and design the good performance materials.

■ ASSOCIATED CONTENT

Supporting Information

Optimized structural parameters with different density functionals, the parallel molecular pairs in supercells used to calculate the electronic couplings, the correlation functions of site energy, and the population propagation of the electron. This material is available free of charge via the Internet at http://pubs.acs.org.

■ AUTHOR INFORMATION

Corresponding Author

*E-mail: yizhao@xmu.edu.cn.

Notes

The authors declare no competing financial interest.

■ ACKNOWLEDGMENTS

This work has been supported by the National Science Foundation of China (Grant Nos. 20833004, 21073146, and 21133007).

■ REFERENCES

(1) Horowitz, G.; Fichou, D.; Peng, X.; Xu, Z.; Garnier, F. *Solid State Commun.* **1989**, *72*, 381−384.
(2) Dimitrakopoulos, C. D.; Malenfant, P. R. L. *Adv. Mater.* **2002**, *14*, 99−117.
(3) Burroughes, J. H.; Bradley, D. D. C.; Brown, A. R.; Marks, R. N.; Mackay, K.; Friend, R. H.; Burns, P. L.; Holmes, A. B. *Nature* **1990**, *347*, 539−541.
(4) Sheats, J. R.; Antoniadis, H.; Hueschen, M.; Leonard, W.; Miller, J.; Moon, R.; Roitman, D.; Stocking, A. *Science* **1996**, *273*, 884−888.
(5) Brabec, C. J.; Sariciftci, N. S.; Hummelen, J. C. *Adv. Funct. Mater.* **2001**, *11*, 15−26.
(6) Hoppe, H.; Sariciftci, N. S. *J. Mater. Res.* **2004**, *19*, 1924−1945.
(7) Murphy, A. R.; Fréchet, J. M. J. *Chem. Rev.* **2007**, *107*, 1066−1096.
(8) Lee, S.; Koo, B.; Shin, J.; Lee, E.; Park, H.; Kim, H. *Appl. Phys. Lett.* **2006**, *88*, 162109.
(9) Pron, A.; Gawrys, P.; Zagorska, M.; Djurado, D.; Demadrille, R. *Chem. Soc. Rev.* **2010**, *39*, 2577−2632.
(10) Mamada, M.; Nishida, J.; Tokito, S.; Yamashita, Y. *Chem. Commun.* **2009**, 2177−2179.
(11) Mamada, M.; Kumaki, D.; Nishida, J.; Tokito, S.; Yamashita, Y. *ACS Appl. Mater. Interfaces* **2010**, *2*, 1303−1307.
(12) Tang, Q.; Liang, Z.; Liu, J.; Xu, J.; Miao, Q. *Chem. Commun.* **2010**, *46*, 2977−2979.
(13) Liang, Z.; Tang, Q.; Liu, J.; Li, J.; Yan, F.; Miao, Q. *Chem. Mater.* **2010**, *22*, 6438−6443.
(14) Brédas, J.-L.; Norton, J. E.; Cornil, J.; Coropceanu, V. *Acc. Chem. Res.* **2009**, *42*, 1691−1699.
(15) Deng, W. Q.; W., A. G., III *J. Phys. Chem. B* **2004**, *108*, 8614−8621.
(16) Yang, X. D.; Li, Q. K.; Shuai, Z. G. *Nanotechnology* **2007**, *18*, 424029.
(17) Nan, G.; Yang, X.; Wang, L.; Shuai, Z.; Zhao, Y. *Phys. Rev. B* **2009**, *79*, 115203.
(18) Zhang, W.; Liang, W.; Zhao, Y. *J. Chem. Phys.* **2010**, *133*, 024501.
(19) Bässler, H. *Phys. Status Solidi B* **1993**, *175*, 15−56.
(20) Movaghar, B.; Grünewald, M.; Ries, B.; Bässler, H.; Würtz, D. *Phys. Rev. B* **1986**, *33*, 5545−5554.
(21) Zhao, Y.; Liang, W. *Chem. Soc. Rev.* **2012**, *41*, 1075−1087.
(22) Troisi, A.; Orlandi, G. *J. Phys. Chem. A* **2006**, *110*, 4065−4070.
(23) Troisi, A.; Cheung, D. L.; Andrienko, D. *Phys. Rev. Lett.* **2009**, *102*, 116602.
(24) Troisi, A. *Chem. Soc. Rev.* **2011**, *40*, 2347−2358.
(25) Hannewald, K.; Bobbert, P. A. *Appl. Phys. Lett.* **2004**, *85*, 1535−1537.
(26) Hannewald, K.; Stojanović, V. M.; Schellekens, J. M. T.; Bobbert, P. A.; Kresse, G.; Hafner, J. *Phys. Rev. B* **2004**, *69*, 075211.
(27) Ishizaki, A.; Tanimura, Y. *J. Phys. Soc. Jpn.* **2005**, *74*, 3131−3134.
(28) Tanimura, Y.; Kubo, R. *J. Phys. Soc. Jpn.* **1989**, *58*, 101−114.
(29) Ishizaki, A.; Fleming, G. R. *Proc. Natl. Acad. Sci. U.S.A.* **2009**, *106*, 17255−17260.
(30) Strümpfer, J.; Schulten, K. *J. Chem. Phys.* **2009**, *131*, 225101.
(31) Wang, D.; Chen, L.; Zheng, R.; Wang, L.; Shi, Q. *J. Chem. Phys.* **2010**, *132*, 081101.
(32) Kondov, I.; Thoss, M.; Wang, H. *J. Phys. Chem. A* **2006**, *110*, 1364−1374.
(33) Kondov, I.; Čížek, M.; Benesch, C.; Wang, H.; Thoss, M. *J. Phys. Chem. C* **2007**, *111*, 11970−11981.
(34) Li, J.; Kondov, I.; Wang, H.; Thoss, M. *J. Phys. Chem. C* **2010**, *114*, 18481−18493.
(35) Makri, N.; Makarov, D. E. *J. Chem. Phys.* **1995**, *102*, 4600−4610.

(36) Makri, N.; Makarov, D. E. *J. Chem. Phys.* **1995**, *102*, 4611−4618.
(37) Makri, N. *J. Math. Phys.* **1995**, *36*, 2430−2457.
(38) Zhao, Y. *J. Theor. Comput. Chem.* **2008**, *7*, 869−877.
(39) Chu, X.; Zhao, Y. *J. Theor. Comput. Chem.* **2009**, *8*, 1295−1307.
(40) Zhong, X.; Zhao, Y. *J. Chem. Phys.* **2011**, *135*, 134110.
(41) Anderson, P. W.; Weiss, P. R. *Rev. Mod. Phys.* **1953**, *25*, 269−276.
(42) Kubo, R. *J. Phys. Soc. Jpn.* **1954**, *9*, 935−944.
(43) Burshtein, A. I. *Zh. Eksp. Teor. Phys.* **1965**, *49*, 1362−1375.
(44) Haken, H.; Reineker, P. *Z. Phys.* **1972**, *249*, 253−268.
(45) Haken, H.; Strobl, G. *Z. Phys.* **1973**, *262*, 135−148.
(46) Goychuk, I.; Hänggi, P. *Adv. Phys.* **2005**, *54*, 525−584.
(47) Si, Y.; Zhong, X.; Zhang, W.; Zhao, Y. *Chin. J. Chem. Phys.* **2011**, *24*, 538−546.
(48) Cheng, Y. C.; Silbey, R. J. *Phys. Rev. A* **2004**, *69*, 052325.
(49) Leggett, A. J.; Chakravarty, S.; Dorsey, A. T.; Fisher, M. P. A; Garg, A.; Zwerger, W. *Rev. Mod. Phys.* **1987**, *59*, 1−85.
(50) Billah, K. Y. R.; Shinozuka, M. *Phys. Rev. A* **1990**, *42*, 7492−7495.
(51) Egorov, S. A.; Everitt, K. F.; Skinner, J. L. *J. Phys. Chem. A* **1999**, *103*, 9494−9499.
(52) Tal-Ezer, H.; Kosloff, R. *J. Chem. Phys.* **1984**, *81*, 3967−3971.
(53) Rossi, M.; Sohlberg, K. *J. Phys. Chem. C* **2009**, *113*, 6821−6831.
(54) Zhang, W.; Zhu, W.; Liang, W.; Zhao, Y.; Nelsen, S. F. *J. Phys. Chem. B* **2008**, *112*, 11079−11086.
(55) Koopmans, T. *Physica* **1934**, *1*, 104−113.
(56) Jordan, K. D.; Paddon-row, M. N. *Chem. Rev.* **1992**, *92*, 395−410.
(57) Cornil, J.; Beljonne, D.; Calbert, J. P.; Brédas, J. L. *Adv. Mater.* **2001**, *13*, 1053−1067.
(58) Datta, A.; Mohakud, S.; Pati, S. K. *J. Mater. Chem.* **2007**, *17*, 1933−1938.
(59) Farazdel, A.; Dupuis, M.; Clementi, E.; Aviram, A. *J. Am. Chem. Soc.* **1990**, *112*, 4206−4214.
(60) You, Z.-Q.; Shao, Y.; Hsu, C.-P. *Chem. Phys. Lett.* **2004**, *390*, 116−123.
(61) Cave, R. J.; Newton, M. D. *Chem. Phys. Lett.* **1996**, *249*, 15−19.
(62) Valeev, E. F.; Coropceanu, V.; da Silva Filho, D. A.; Salman, S.; Brédas, J. L. *J. Am. Chem. Soc.* **2006**, *128*, 9882−9886.
(63) Coropceanu, V.; Cornil, J.; da Silva Filho, D. A.; Olivier, Y.; Silbey, R.; Brédas, J.-L. *Chem. Rev.* **2007**, *107*, 926−952.
(64) Huang, J.; Kertesz, M. *Chem. Phys. Lett.* **2004**, *390*, 110−115.
(65) Frisch, M. J.; Trucks, G. W.; Schlegel, H. B.; Scuseria, G. E.; Robb, M. A.; Cheeseman, J. R.; Scalmani, G.; Barone, V.; Mennucci, B.; Petersson, G. A.; et al. *Gaussian 09*, Revision A.1; Gaussian, Inc.: Wallingford, CT, 2009.
(66) Ponder, J. W. *TINKER: Software Tools for Molecular Design*, 5.1 ed.;Washington University School of Medicine: Saint Louis, MO, 2010.
(67) Ponder, J. W.; Richards, F. M. *J. Comput. Chem.* **1987**, *8*, 1016−1024.
(68) Ren, P.; Ponder, J. W. *J. Phys. Chem. B* **2003**, *107*, 5933−5947.
(69) Jorgensen, W. L.; Maxwell, D. S.; Tirado-Rives, J. *J. Am. Chem. Soc.* **1996**, *118*, 11225−11236.
(70) Cheung, D. L.; Troisi, A. *J. Phys. Chem. C* **2010**, *114*, 20479−20488.
(71) Vehoff, T.; Baumeier, B.; Troisi, A.; Andrienko, D. *J. Am. Chem. Soc.* **2010**, *132*, 11702−11708.
(72) Newton, M. D.; Sutin, N. *Annu. Rev. Phys. Chem.* **1984**, *35*, 437−480.
(73) Nelsen, S. F.; Blackstock, S. C.; Kim, Y. *J. Am. Chem. Soc.* **1987**, *109*, 677−682.
(74) Wang, L. J.; Li, Q. K.; Shuai, Z. G.; Chen, L. P.; Shi, Q. *Phys. Chem. Chem. Phys.* **2010**, *12*, 3309−3314.
(75) Marcus, R. A. *Rev. Mod. Phys.* **1993**, *65*, 599−610.
(76) Marcus, R. A.; Sutin, N. *Biochem. Biophys. Acta* **1985**, *811*, 265−322.
(77) Bixon, M.; Jortner, J. *J. Phys. Chem.* **1986**, *90*, 3795−3800.
(78) Zhao, Y.; Liang, W. Z.; Nakamura, H. *J. Phys. Chem. A* **2006**, *110*, 8204−8212.
(79) Zhu, W.; Zhao, Y. *J. Chem. Phys.* **2007**, *126*, 184105.